First Principles Study of Neutral and Anionic (Medium-Size) Aluminum Nitride Clusters: Al_nN_n, $n = 7-16$

Aurora Costales,*,† M. A. Blanco,† E. Francisco,† A. Martín Pendás,† and Ravindra Pandey‡

Departamento de Química Física y Analítica, Facultad de Química, Universidad de Oviedo, 33006 Oviedo, Spain, and Department of Physics, Michigan Technological University, Houghton, Michigan 49931

Received: November 14, 2005; In Final Form: December 27, 2005

We report the results of a theoretical study of Al_nN_n ($n = 7-16$) clusters that is based on density functional theory. We will focus on the evolution of structural and electronic properties with the cluster size in the stoichiometric AlN clusters considered. The results reveal that the structural and electronic properties tend to evolve toward their respective bulk limits. The rate of evolution is, however, slow due to the hollow globular shape exhibited by the clusters, which introduces large surface effects that dominate the properties studied. We will also discuss the changes induced upon addition of an extra electron to the respective neutral clusters.

1. Introduction

The semiconductor industry has uninterruptedly grown during the past few decades. After the exhaustive exploration of the electronic properties of silicon, the need for new materials with different properties has drawn a lot of attention to nanoscale aluminum nitride semiconductor structures. The electronic properties of AlN make it suitable for the fabrication of light-emitting diodes and a new generation of short-wavelength lasers. It also has multiple applications in microelectronic components for high-temperature and high-power devices.[1]

Though this material has been studied extensively in the solid state and thin film forms, research at the micro- and nanocluster levels is still lacking. Representing a link between the solid state and the isolated molecular world, a theoretical study of these clusters with different sizes has drawn increasing attention during recent years.[2−15] Recent experimental studies on gaseous AlN, involving infrared spectroscopy, mass spectra, and Knudsen cell mass spectrometry, showed the existence of a large diversity of neutral and charged species.[6,10,16] Our calculations[7,8,11,12,17,18] based on the density functional theory (DFT) allow us to predict the structure and some properties of the clusters, which can be compared with the experimental observations. A match between the predicted and observed properties identifies the correct structure. In some cases, the predicted properties help experimentalists to interpret their results.

Keeping in mind the link between the two worlds that the cluster level represents, we continue in this work the study of the evolution of cluster properties with size, to determine the limit in which the bulk behavior is reached. We also analyze in this work the changes induced upon addition of an extra electron to the neutral clusters. Our previous electronic structure calculations on smaller clusters,[7,8,11,12,17,18] and our atomistic exploration of the potential energy surface of a larger range of clusters[19] are used both to generate plausible isomer configurations and to gain insights on the evolution of properties with size.

We have organized the rest of the paper as follows. The computational scheme used in this work is presented in section 2. The generation and selection of the different isomers is described in section 3. In section 4, we present and discuss our results, the evolution of different cluster properties with size for both neutral and anionic clusters. Finally, we present our conclusions in section 5.

2. Computational Scheme

Electronic structure calculations were performed on neutral and anionic aluminum nitride clusters, Al_nN_n, $n = 7-16$, using the Gaussian 98 code.[20] All electron calculations were carried out by solving the Kohn−Sham equations in the framework of the DFT. The generalized gradient approximation (GGA) was used in all calculations, using the gradient-corrected exchange functional of Becke[21] and the gradient-corrected Perdew−Wang[22] correlation functional form (BPW91). The 6-31G** basis set was employed to describe the aluminum and nitrogen atoms. For anionic systems, diffuse basis sets are usually expected to play an important role in determining the structural configuration. However, we have previously analyzed the effect of diffuse functions in small anionic AlN clusters,[17] obtaining small, nonsignificant variations in the structural properties. This fact, along with the increase in the computational time when diffuse functions are included and our aim of comparing the present data with previous results[17,18] on the same footing, leads us to use the 6-31G** basis set.

All of the isomers analyzed in this study have been fully geometrically optimized by employing analytic gradients and updated Hessians, with a convergence criteria of 10^{-4} hartree/Å and 10^{-9} hartree for gradients and energies, respectively. The stability of the lowest energy isomers has been checked by computation of the vibrational frequencies under the harmonic approximation, with analytical force constants.

3. Configurational Isomer Selection

The choice of different structures and geometries as starting points to perform the optimization process is relatively simple when the number of atoms in the cluster is small. In this case, we can employ visual inspection to suggest all of the possible structural conformers. However, the selection of the initial structural isomers becomes the main problem when the cluster

* Author to whom correspondence should be addressed. E-mail: yoyi@carbono.quimica.uniovi.es.
† Universidad de Oviedo.
‡ Michigan Technological University.

10.1021/jp056569+ CCC: $33.50
Published on Web 02/07/2006

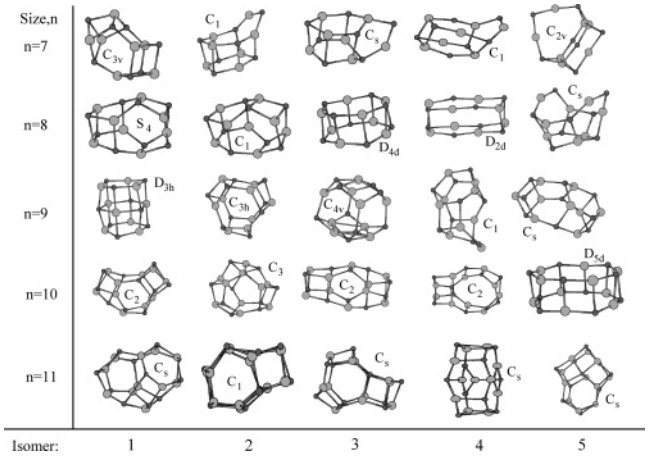

Figure 1. Schematic representation of the different isomers considered in this study for $n = 7-11$. Nitrogen atoms are represented by small dark circles, and aluminum atoms by light large circles. Point symmetry labels for the isomers are shown.

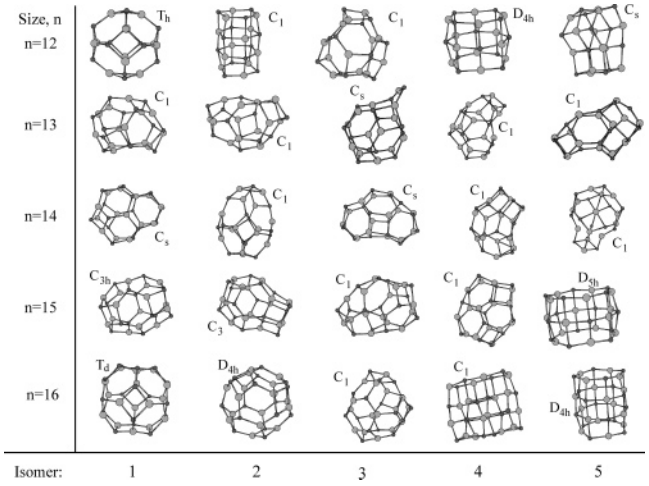

Figure 2. Schematic representation of the different isomers considered in this study for $n = 12-16$. Nitrogen atoms are represented by small dark circles, aluminum atoms by light large circles. Point symmetry labels for the isomers are shown.

size increases. The need to carry out an exhaustive exploration of the geometrical configuration space to locate the lowest energy isomer is computationally costly and extremely difficult. To this effort, we present the following strategy: (i) We explore the potential energy surface to obtain the different structural isomers using our cluster code.[23] This is an atomistic program in which we describe the interactions among the different atoms in the cluster by means of a simple Born−Mayer-like potential. This allows us to generate thousands of conformers or stable configurations of a given molecular complex by means of a Monte Carlo basin hopping global minimization method (see details in ref 19). (ii) We select the five lowest energy isomers obtained in the atomistic simulation for each size and use them as starting points in the density functional optimization procedure. In this way, we may perform a global optimization of medium to large AlN clusters in two steps, an initial thorough exploration using a lower-quality energy surface, and a final high-quality energy surface analysis of the selected configurational low-energy regions. Nevertheless, the tasks are still quite costly in terms of CPU time: The DFT local optimization of the five lowest atomistic energy isomers of $Al_{15}N_{15}$ took almost 16 days of CPU time, while the complete atomistic global optimization, comprising 10 000 individual local optimizations, took less than 25 min of CPU time.

4. Results and Discussion

In this section, we present the most relevant features of the lowest energy isomers for neutral and anionic clusters and discuss the evolution of several properties with the cluster size. We have classified the properties into six categories, each one corresponding to a different subsection: structural, energetic, geometric, coordination, vibrational, and electronic properties.

A. Structural Properties. Figures 1 and 2 display schematic pictures of the different isomers considered in this study along with their symmetry point groups. The energies relative to the most stable isomer of the optimized structures are collected in Table 1. The conformers employed as starting points in the optimization procedure were taken from the cluster output as described in section 3. To test the reliability of our procedure, we compare the agreement between the atomistic[19] prediction of the lowest energy isomer and the prediction obtained within the density functional scheme. The agreement between these two methodologies is almost complete in this series, the only exceptions being Al_8N_8 and $Al_{14}N_{14}$. In these two cases, the relative ordering of the lowest two isomers is reversed, with the lowest DFT energy isomer becoming the second-lowest atomistic energy isomer and vice versa.

TABLE 1: Energy Relative to the Most Stable Isomer (in eV) of the Optimized Stable Configurations of Aluminum Nitride Clusters

		neutral	anion		neutral	anion
isomer		E (eV)	E (eV)		E (eV)	E (eV)
1	Al_7N_7	0.00	0.00	$Al_{12}N_{12}$	0.00	0.00
2		0.12	0.46		1.94	1.71
3		0.48	0.85		2.62	2.78
4		0.78	0.59		2.91	2.39
5		1.55	1.83		2.98	2.17
1	Al_8N_8	0.00	0.88	$Al_{13}N_{13}$	0.00	0.02
2		0.0004	0.002		0.03	0.00
3		0.65	1.06		0.41	0.51
4		1.44	0.00		0.84	1.09
5		2.32	2.03		1.06	0.80
1	Al_9N_9	0.00	0.22	$Al_{14}N_{14}$	0.00	0.64
2		0.02	0.00		0.52	0.00
3		1.10	1.05		0.87	0.77
4		2.14	2.25		0.95	0.87
5		2.50	1.96		0.95	0.51
1	$Al_{10}N_{10}$	0.00	0.06	$Al_{15}N_{15}$	0.00	0.00
2		0.09	2.11		0.27	2.11
3		0.65	1.00		1.61	1.00
4		0.99	0.44		1.62	0.44
5		1.86	0.00		4.59	0.00
1	$Al_{11}N_{11}$	0.00	0.00	$Al_{16}N_{16}$	0.00	0.00
2		1.02	1.37		0.50	1.37
3		1.36	1.04		2.45	1.04
4		1.38	1.24		2.75	1.24
5		1.58	1.59		3.02	1.59

To validate the atomistic results, we have also compared them[19] with those obtained in previous density functional calculations in small clusters ($n = 1-6$).[7,8,11,12,17,18,24] The structures of the lowest energy isomers found in both calculations were the same, the only mismatch being Al_5N_5. While a numerical basis-set calculation[8] gives the D_{5h} planar ring also found as the atomistic lowest-energy isomer, with a C_s AlN-capped cube being second in energy in both cases, the situation was reversed when an analytical basis set was used in the DFT calculation.[18] In all cases, the two isomers were close, their energy differences being 0.78 (atomistic), 0.39 (numerical basis

set DFT), and −0.06 eV (analytic basis set DFT). This illustrates that, although the energy differences can change in different methods, they will generally provide the same energy ordering except in cases close to degeneracy.

The strong preference for aluminum−nitrogen alternate bonds together with an unambiguous trend toward three-dimensional (3D) structures predicted for Al_5N_5[18] is maintained in the larger clusters. This is one of the needed steps in reaching bulklike behavior. In the cluster series, we find a strong competition between two structural motifs: the Al_2N_2 planar square and the planar or chairlike hexagonal Al_3N_3 group. With these two building blocks, two different crystalline structures can be constructed: The first leads to the B1 or NaCl-type crystalline structure, while the second one is the brick to build the B3 or B4 crystalline nets. Since AlN appears at normal conditions in the B4 structure, a high number of hexagons in the clusters may be tentatively related with a progression toward bulklike behavior. Figures 1 and 2 show an increasing trend in the number of hexagons over squares for the most stable conformer. With the increase in the cluster size, open structures formed by six- or higher-membered rings are preferred over closed ones, e.g., cubelike structures with six- and four-membered rings. The symmetry of these isomers is linked to their structural types. In this way, rings and stacked rings display high-order symmetry axes, while cages present lower symmetries except for some particular sizes, T_h and T_d when $n = 12$ and 16, respectively, and C_{3v} and C_{3h} for $n = 7$ and 15, respectively, in their corresponding lowest energy isomers. The mixture of the different elements present in these clusters deprives them of symmetry.

We can compare our results for the neutral clusters with the work of Wu et al.[14] The agreement is excellent, with Al_9N_9 and $Al_{10}N_{10}$ being the only exceptions, since the Wu et al. global minima are predicted as our second isomers in these cases. Specifically, these isomers are quasi-degenerate in energy, as we show in Table 1. It is important to note that Wu and co-workers have employed a particular model to build the cluster, since their main aim is to generate aluminum nitride cages. They fixed the maximum coordination number as three. In our exploration of the potential energy surface no restrictions were imposed. In this way, the 4-fold coordination index reached in Al_9N_9 may explain the alteration in the energy ordering.

The addition of an electron to the neutral cluster does not induce significant structural changes in most of the isomers analyzed in this work. The configurational symmetry of the lowest energy isomer is maintained, except for $n = 8$, 9, 10, 13, and 14. The added electron makes $Al_8N_8^-$ transform into a more symmetric structure, D_{2d} (the fourth isomer in the neutral case), whose building blocks are squares. This structure is almost degenerate in energy with isomer 2 (the second lowest energy isomer in the neutral case). In the $Al_9N_9^-$ cluster, the ordering of the first two isomers is changed, and so the predicted lowest-energy neutral cluster of Wu et al. is our lowest energy anion. An important effect is that the addition of an electron breaks the degeneration between these two conformers. Relatively larger structural changes are produced when an electron is added to $Al_{10}N_{10}$. The lowest energy structure is a more symmetric structure, D_{5d} drumlike, which corresponds to the fifth isomer in the neutral case. The minimum for $Al_{10}N_{10}^-$ is almost degenerate with the next conformer, this being the lowest energy isomer for the neutral cluster. The addition of an electron to $Al_{13}N_{13}$ does not break the degeneracy between the two lowest energy structures, but it changes the relative ordering between them. For $Al_{14}N_{14}^-$, the lowest energy isomer is the second one in the corresponding neutral charge state. In this cluster, a large alteration of the relative energy ordering happens with respect to the neutral cluster.

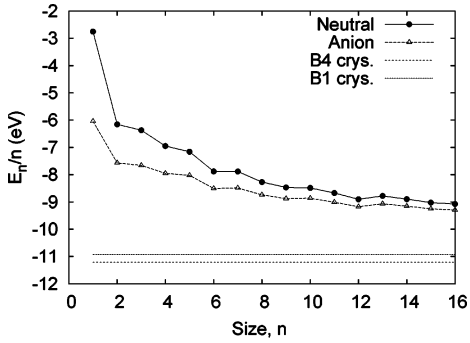

Figure 3. Binding energy per molecule, E_n/n (in eV), versus the number of AlN units in the cluster, n.

B. Energetic Properties. The stability of neutral and anionic aluminum nitride clusters with respect to their constituent atoms can be characterized by their binding energy, $E_n = E(Al_nN_n) - nE(Al) - nE(N)$ in the neutral case, whereas in the anionic clusters the negative charge is assigned to a N atom in the atomic references, since N is more electronegative than Al. In Figure 3, we have plotted the binding energy per molecule, E_n/n, as a function of the number of AlN units in the cluster, n. To improve the visualization of the evolution of all properties with the cluster size, we include the values obtained for small clusters in our previous works.[17,18] E_n/n displays the expected behavior, in both neutral and anionic systems: an asymptotic decrease when the cluster size increases. The slope of these curves is large for the small cluster sizes, whereas from $n \simeq 9$ the curve is almost flat with a small decrease of the binding energy per molecule with the cluster size. This indicates an approach to the stationary bulk regime.

The evolution of the binding energy per molecule with the cluster size is similar for the anionic clusters, although presenting lower values. This behavior is expected, because the anionic clusters are more stable than the neutral nanoaggregates. It is to be noted that both neutral and ionic binding energies seem to have a periodic steplike behavior, so that odd n values have lower energy gains when compared to even n values upon increasing n. This is not an electronic effect, since all neutral clusters are closed-shell systems with an even number of electrons, while all anions have an odd number of electrons; despite this, both show the same alternating behavior, since their lowest-energy structures are the same in most cases. Thus, this must be related to the odd−even number of Al−N pairs, allowing for a given number of four- or six-membered rings. Nonetheless, this behavior changes for $n \geq 9$, as shown below for the second energy differences.

We have also plotted in Figure 3 the values for the binding energy in the neutral B4 and B1 crystal limits. In this way, we can see that the bulk regime is still around 2 eV per unit less in energy. The simulations of the B4 and B1 solid-state phases have been performed using the crystal98 code.[25] The crystalline phases have been described employing the same density functional forms and the same basis sets to compare them on the same footing. During the crystalline optimization procedure, we found a well-known basis set linear dependence due to the low value of the diffuse exponent in the aluminum basis set. This exponent was changed from 0.0556577 in the cluster calculations to 0.08 in the crystalline calculations. We have analyzed the influence of the outermost exponent over the different crystalline properties, noticing very small changes in the properties.

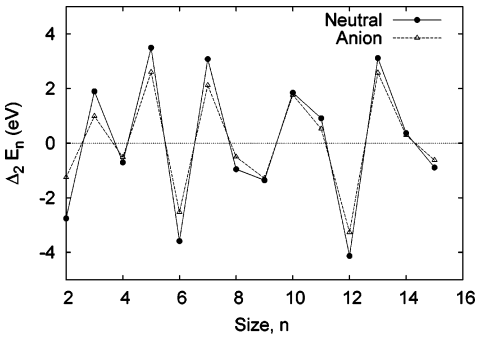

Figure 4. Second energy difference, $\Delta_2 E_n$ (in eV), versus cluster size, n.

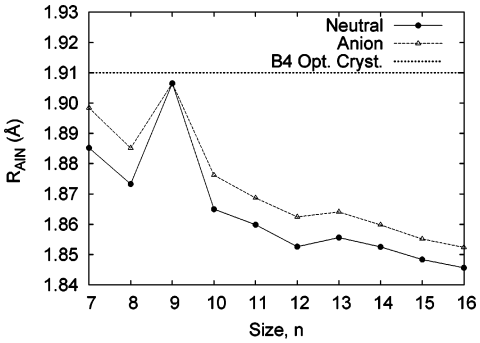

Figure 5. Average first neighbor distance (R_{AlN}, in Å) versus the number of AlN units, n. The horizontal line displays the values for the solid state, B4 phase.

In Figure 4, we plot the second energy difference $\Delta_2 E_n = 2E_n - E_{n-1} - E_{n+1}$ versus the cluster size for neutral and anionic systems. Both cluster types present the same trends. Several sizes exhibit negative values for this magnitude, linked to clusters containing a particular number of molecules that are more stable than their immediate neighbors. We find such a behavior for $n = 4$, 6, 8, 9, 12, and 15. At $n = 4$ the planar octagonal (neutral) and the cubic (anion) structures are slightly more stable than their neighboring global minima at $n = 3$ and 5. The isomer with $n = 6$ is particularly more stable than their neighbors. It is a drumlike structure, formed by two hexagons linked by bonds with a coordination index of 3. The $n = 8$ cluster is again barely more stable than those with $n = 7$ and 9, most likely due to the instability of $n = 7$, since $n = 9$ is even more stable. The latter is exceptionally stable and displays a structure of piled hexagonal rings, which has already been shown to be highly stable by atomistic calculations.[19] Its anionic form shows a cage structure with a high number of hexagons. For the $n = 12$ neutral and anionic AlN clusters, the key to their stability is the formation of cage structures, very symmetric, with a high number of hexagons as building blocks. The same goes for $n = 16$, but we cannot advance unambiguously the trend, since values for $n = 17$ are lacking. Regarding the $n = 15$ cluster, it is also of high symmetry and has a quite regular hexagonal grid. However, $\Delta_2 E_n$ measures also its stability with respect to $n = 16$, of even higher symmetry, and thus its value is not so low as $n = 12$ and $n = 6$. All of these cluster sizes, related with particularly stable structures, are usually considered as magic numbers.

C. Geometric Properties. We start the discussion of the geometric properties of our clusters by presenting the evolution of the average first neighbor distance with cluster size. These values are displayed in Figure 5. A parallel behavior for the neutral and anionic clusters is observed. As expected the latter present larger distances than the former, since the extra electron induces a redistribution of the electron density, making the atoms move away from each other to reduce the electrostatic repulsion. As a general trend, we can appreciate a decrease in the average first neighbor distance with cluster size, Al_9N_9 being the most important exception.

This trend is a little bit unexpected if we compare these values with the average aluminum−nitrogen distances in the solid state, 1.91 Å for the B4 phase and 2.05 Å for the B1 phase, both values computed as described in the previous subsection. This apparent discrepancy in the evolution of the first neighbor distances with cluster size is due to the hollow globular structure of the lowest energy isomers. For these, surface effects are larger, shortening the average aluminum−nitrogen distance. This fact indicates that the bulk behavior has not been reached yet. The clusters should evolve from the hollow globular forms with 3-fold coordination to adopt 3D structures that fill the cluster with 4-fold coordinated atoms. This coordination is already shown by the neutral Al_9N_9 cluster, making its first neighbor distance larger than the rest (although the coordination is almost square, not tetrahedral, and the structure of the anion is again globular with 3-fold coordination).

Several relationships between the principal moments of inertia are indicative of the shape of the cluster. If the asymmetry parameter λ, defined as $(I_a + I_b - I_c)/I_c$ (where a, b, and c are the principal inertia axes, ordered so that $I_a \leq I_b \leq I_c$) is equal to 0, then the cluster is planar. When $\lambda = 1$ the cluster is a spherical top. If $I_a = 0$ and $\lambda = 0$, then the cluster is linear. Spherical-like clusters should present large λ values, while planarlike clusters should show small λ values. We plot the values of λ for the neutral and anionic aluminum nitride clusters in Figure 6. We can observe that two sizes, $n = 12$ and $n = 16$, have $\lambda = 1$ (T_d and T_h symmetries). We have found neither planar nor linear clusters in this study. All other λ values range between 0.5 and 0.6 (except for the quite symmetric $n = 9$ and $n = 15$ clusters), indicating that they are globular but asymmetric.

As done in ref 19, we define an effective radius for the cluster using the moments of inertia, taking their average as defining a solid sphere equivalent to the cluster, $^2/_5 MR_{eff}^2 = {}^1/_3(I_a + I_b + I_c)$. This effective radius is plotted in Figure 7 and proves to be quite independent of the charge state of the clusters, the small difference for particular sizes being a direct consequence of the large difference in their lowest energy structures (particularly for $n = 10$) respective moments of inertia. We also plot an estimation of the effective radii of an equivalent spherical portion of the B4 phase. This estimation assumes that the density of atoms in the sphere is the same as that in the corresponding solid (optimized using the current basis sets and density functionals). We have corrected this radius by subtracting half of the interatomic distance, to account for the different definitions (according to nuclear positions in the clusters, according to atomic volumes and radii in the solid-state estimation). The correlation is remarkable, given the hollow globular shapes of the clusters, and may be hinting that the lack of internal atoms emanates from a lack of room rather than from other energetic considerations.

We show the differences in the average distance relative to the center of mass, $\Delta R_{rel} = R_{rel}^N - R_{rel}^{Al}$, in the insert of Figure 7. This difference is positive, indicating a trend of the nitrogen atoms to escape away from the center of mass that is not present for the Al atoms. When the evolution of ΔR_{rel} is compared with size for neutral and anionic clusters, it is observed that the anionic clusters present higher values than the neutral ones. This points out that the extra electron is mainly shared by the N

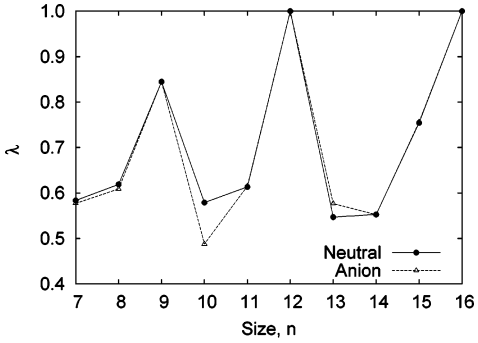

Figure 6. Asymmetry parameter (λ, adimensional) of the principal moments of inertia versus the number of AlN units in the cluster, *n*.

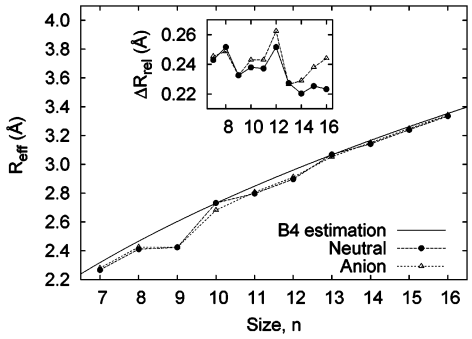

Figure 7. Effective radius of the cluster (R_{eff}, in Å) versus the number of AlN units, *n*. The solid line represents a spherical average of the B4 phase. The insert shows the difference in average distances to the center of mass, ($\Delta R_{rel}^{N} - R_{rel}^{Al}$, in Å), versus *n*.

atoms, making them repel each other even more. This is in agreement with the electronegativity values and previous results in small clusters.[17,18]

D. Coordination Index. The coordination index is quite a revealing property to evaluate the convergence toward the bulk limit. In the solid state, aluminum nitride crystallizes in the B4 phase, and all of the atoms show a coordination index of four in a tetrahedral environment. The lowest energy isomers studied in this work show a coordination index equal to three for all atoms involved in the structure, the only exception being the neutral Al_9N_9, which presents 66.6% of atoms with 3-fold coordination and 33.3% with a 4-fold coordination. However, this is not exactly a bulklike coordination. Although in the B4 phase the atoms constitute layers of six-membered rings stacked on top of each other like in Al_9N_9, the interlayer bonds alternate, each atom bonding to only one layer, instead of bonding to both layers as happens in Al_9N_9. Thus, the 4-fold coordination is achieved here with two interlayer bonds, since the hexagonal sheet is limited to a single hexagon layer.

Again, the coordination index indicates that the bulklike behavior is still far away, even though the approaching direction seems to be the correct one since the N−N bonds present in some of the low-energy isomers of sizes $n = 1-6$[17,18] have disappeared, and only some higher-energy isomers present 2-fold coordinations for $n = 7$, 8, 9, and 13.

E. Vibrational Properties. To confirm the stability of the optimized lowest energy isomers, harmonic vibrational frequencies have been computed for the neutral and anionic Al_nN_n clusters. Their values are displayed in Figure 8. The vibrational frequencies of these clusters range from 97 to 970 cm^{-1}. It is no longer possible to make a clear separation of the spectra (let us recall that, in the $n = 1-6$ lowest energy isomers, the spectra could be separated in two regions: the lower one, corresponding to the bending and torsion movements, and the higher region,

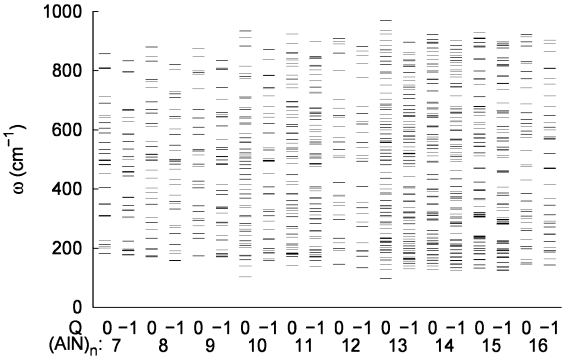

Figure 8. Vibrational frequency spectra versus the number of units AlN in the cluster for the neutral and anionic clusters.

which involved the stretching of the Al−N bonds). In the present case the high number of atoms in the clusters introduces a large amount of coupling between vibrational modes.

Figure 8 clearly reflects those clusters that underwent structural changes upon adding an electron to the neutral ones, with a corresponding qualitative change in the vibrational spectra. When the neutral and the anionic cluster exhibit the same lowest energy conformer, it is easy to appreciate that the anionic cluster always presents lower vibrational frequency values, in agreement with the higher interatomic distances exhibited by the charged clusters. All of this is in contrast with the expected bulklike behavior. The spectra should split in acoustic and optical branches,[26] the former starting at $\omega = 0$, being mostly insensitive to the addition of electrons or to surface reorganization. Thus, the vibrational properties are expected to converge very slowly to the bulk behavior.

F. Electronic Properties. Both adiabatic and vertical values for the electron affinity (EA) and vertical ionization potential (VIP) for the lowest energy isomers of the aluminum nitride clusters were computed in this study as follows: $EA = E_{Q=0} - E_{Q=-1}$, $IP = E_{Q=+1} - E_{Q=0}$, where E is the total energy of the cluster and Q its charge. From Schaefer et al.,[27] the vertical electron affinity (VEA, also called vertical detachment VDE) is defined as the energy difference between the anionic and neutral clusters when both are at the anionic optimized geometry, while the adiabatic electron affinity (AEA) is defined as the energy difference between the neutral and anionic clusters at their optimized geometries. The vertical attachment energy (VAE) has also been computed, defined as the energy difference between the neutral and anionic clusters with both at the neutral cluster optimized geometry. Although the vertical attachment energy is not currently measured through any experiment, it provides a lower bound to the AEA in the same way as the VDE is an upper bound to it.[27] The vertical ionization potential (VIP) is defined as the energy difference between the cationic and neutral clusters, both at the neutral optimized geometry.

The calculated values of the above quantities for the Al_nN_n clusters are displayed in Figure 9. The relative ordering of the VAE, AEA, and VDE is as expected. It is observed that the electron affinity decreases when the cluster size increases. Particularly small values are exhibited by the symmetric clusters with $n = 12$ and $n = 15$, although the $n = 16$ cluster, also of high symmetry, does not seem to be abnormally small.

The overall trend of the electron affinity with the cluster size is interesting. Neumark's group, several years ago, obtained the bulk electron affinity for GaP using a linear fit of the electron affinity of five large clusters.[28] They took into account that the photoelectron spectroscopy of metals, semiconductors, and weakly bound clusters generally shows that the electron affinity

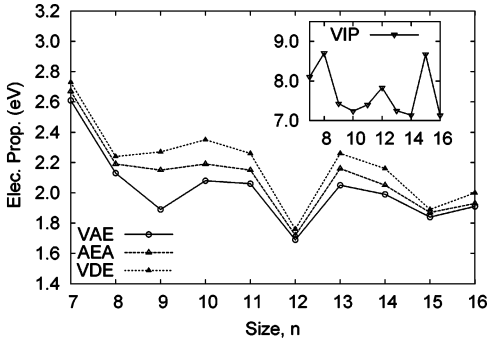

Figure 9. Vertical detachment energy (VDE), adiabatic electron affinity (AEA), and vertical attachment energy (VAE) versus the number of AlN units in the cluster. The inset presents the vertical ionization potential versus the cluster size. All energies are given in eV.

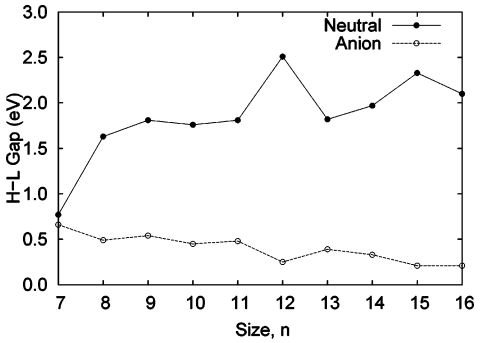

Figure 10. HOMO−LUMO gap versus the number of AlN units in the cluster.

changes smoothly with the cluster size and extrapolates correctly to the bulk value. In this way, we can estimate the electron affinity of bulk AlN according to the relationship $EA_{bulk} = E_i - E_g$, where E_i is the bulk ionization (also called the work function) and E_g is the band gap. The measured value for the work function in the B4 wurzite phase of AlN is 5.35 eV.[29] This value has been measured at high temperatures, but its temperature dependence is usually small. The value of the band gap in the same phase for the AlN solid is 6.23 eV.[30] Taking these two values, the estimated bulk electron affinity for the wurzite AlN is 0.88 eV. Our results show an oscillatory behavior of the electron affinity with an increase in the cluster size, and hence it is necessary to increase the cluster size to reach the bulk behavior or at least to perform a meaningful extrapolation. It is also important to notice that AlN is a promising material for field emitters because electrons in materials with nearly zero electron affinity can be easily extracted from the surface into a vacuum by a small electric field.[31,32]

In the inset of Figure 9 we present the evolution of the vertical ionization potential with the cluster size. It is observed that VIP is decreasing when the number of AlN units in the cluster increases. This magnitude should be compared in the bulk with the work function, 5.35 eV[29] for AlN in the B4 phase. The trend is again correct, but the value is still far away from the bulk value. Again, this electronic property is indicating that the bulk behavior has not been reached yet. The clusters with $n = 12$, 8, and 15 show higher values for the VIP.

The computed highest occupied molecular orbital (HOMO)−lowest unoccupied molecular orbital (LUMO) gap results for the neutral and anionic Al_nN_n clusters are depicted in Figure 10. As expected the neutral clusters show a higher value of the HOMO−LUMO gap than the anionic clusters, since all neutral clusters display closed shell electronic configurations. It is interesting to see that the behavior of the HOMO−LUMO gap correlates very well with the difference between the ionization potential and the electron affinity on the basis of Koopman's theorem. In the bulk limit, we should compare this magnitude with the band gap (6.23 eV). This value is much higher than the values exhibited by these clusters, and it may indicate that the bulk limit behavior is even more ionic than that in these clusters.

5. Conclusions

The results of this work show that many structural and energetic properties of the stoichiometric Al_nN_n clusters evolve in the medium size range ($n = 7-16$), following trends compatible with bulk behavior at $n \rightarrow \infty$. Nevertheless, this bulk limit is still far from our computed results, probably due to the dominance of hollow globular conformers with large surface effects in this size region. Further increases in the cluster size allowing for the appearance of alternate stackings of hexagons may be an important step to reproduce the bulk behavior of AlN.

Acknowledgment. We thank S. Gowtham for helpful discussions. This research has been funded by the Spanish Ministerio de Ciencia y Tecnología, grant BQU2003-06553. A.C. thanks the Spanish Ministerio de Ciencia y Tecnología for her Ramón y Cajal position.

References and Notes

(1) Nakamura, S. In *Proceedings of the International Symposium on Blue Laser and Light Emitting Diodes*; Yoshikawa, A., Kishino, K., Kobayashi, M., Yasuda, T., Eds.; Chiba University Press: Japan, 1996; p 119.
(2) BelBruno, J. J. *Chem. Phys. Lett.* **1999**, *313*, 795.
(3) Boo, B. H.; Liu, Z. *J. Phys. Chem. A* **1999**, *103*, 1250−1254.
(4) BelBruno, J. J. *Heteroat. Chem.* **2000**, *11*, 281.
(5) Wu, H.; Zhang, C.; Xu, X.; Zheng, L.; Zhang, Q. *Sci. China., Ser. B: Chem.* **2000**, *43*, 634−642.
(6) Andrews, L.; Zhou, M.; Chertihin, G. V.; Bare, W. J.; Hannachi, Y. *J. Phys. Chem. A* **2000**, *104*, 1656.
(7) Kandalam, A. K.; Pandey, R.; Blanco, M. A.; Costales, A.; Recio, J. M.; Newsam, J. M. *J. Phys. Chem. B* **2000**, *104*, 4361.
(8) Kandalam, A. K.; Blanco, M. A.; Pandey, R. *J. Phys. Chem. B* **2001**, *105*, 6080.
(9) Chang, C.; Patzer, A. B. C.; Sedlmayr, E.; Steinke, T.; Sülzle, D. *Chem. Phys. Lett.* **2001**, *271*, 283−292.
(10) Leskiw, B. D.; Castleman, A. W., Jr.; Ashman, C.; Khanna, S. N. *J. Chem. Phys.* **2001**, *114*, 1165−1169.
(11) Kandalam, A. K.; Blanco, M. A.; Pandey, R. *J. Phys. Chem. B* **2002**, *106*, 1945−1953.
(12) Costales, A.; Blanco, M. A.; Martín Pendás, A.; Kandalam, A. K.; Pandey, R. *J. Am. Chem. Soc.* **2002**, *124*, 4116.
(13) Sun, Q.; Wang, Q.; Gong, X. G.; Kumar, V.; Kawazoe, Y. *Eur. Phys. J. D* **2002**, *18*, 77−81.
(14) Wu, H.; Zhang, F.; Xu, Z.; Zhang, X.; Jiao, H. *J. Phys. Chem. A* **2003**, *107*, 204−209.
(15) Li, Y.; Brenner, D. W. *Phys. Rev. Lett.* **2004**, *92*, 0755031.
(16) Meloni, G.; Gingerich, K. A. *J. Phys. Chem.* **2000**, *113*, 10978.
(17) Costales, A.; Pandey, R. *J. Phys. Chem. A* **2003**, *107*, 191−197.
(18) Costales, A.; Kandalam, A. K.; Pandey, R. *J. Phys. Chem. B* **2003**, *107*, 4508−4514.
(19) Costales, A.; Blanco, M. A.; Francisco, E.; Pandey, R.; Martín Pendás, A. *J. Phys. Chem. B* **2005**, *109*, 24352−24360
(20) Frisch, M. J.; Trucks, G. W.; Schlegel, H. B.; Scuseria, G. E.; Robb, M. A.; Cheeseman, J. R.; Zakrzewski, V. G.; Montgomery, J. A., Jr.; Stratmann, R. E.; Burant, J. C.; Dapprich, S.; Millam, J. M.; Daniels, A. D.; Kudin, K. N.; Strain, M. C.; Farkas, O.; Tomasi, J.; Barone, V.; Cossi, M.; Cammi, R.; Mennucci, B.; Pomelli, C.; Adamo, C.; Clifford, S.; Ochterski, J.; Petersson, G. A.; Ayala, P. Y.; Cui, Q.; Morokuma, K.; Malick, D. K.; Rabuck, A. D.; Raghavachari, K.; Foresman, J. B.; Cioslowski, J.; Ortiz, J. V.; Stefanov, B. B.; Liu, G.; Liashenko, A.; Piskorz, P.; Komaromi, I.; Gomperts, R.; Martin, R. L.; Fox, D. J.; Keith, T.; Al-Laham, M. A.; Peng, C. Y.; Nanayakkara, A.; Gonzalez, C.; Challacombe, M.; Gill, P. M. W.; Johnson, B. G.; Chen, W.; Wong, M. W.; Andres, J. L.; Head-Gordon, M.; Replogle, E. S.; Pople, J. A. *Gaussian 98*; Gaussian, Inc.: Pittsburgh, PA, 1998.
(21) Becke, A. D. *Phys. Rev. A* **1988**, *38*, 3098.
(22) Perdew, J. P.; Wang, Y. *Phys. Rev. B* **1992**, *45*, 13244.

(23) Francisco, E. *The cluster Program*; Universidad de Oviedo: Oviedo, Spain, 2001−2004.
(24) Costales, A.; Kandalam, A. K.; Martín Pendás, A.; Blanco, M. A.; Recio, J. M.; Pandey, R. *J. Phys. Chem. B* **2000**, *104*, 4368−74.
(25) Saunders, V. R.; Dovesi, R.; Roetti, C.; Causà, M.; Harrison, N. M.; Orlando, R.; Zicovich-Wilson, C. M. *crystal98 User's Manual*; University of Torino: Torino, Italy, 1998.
(26) Grossner, U.; Furthmüller, J.; Beschstedt, F. *J. Electron. Mater.* **2000**, *29*, 281.
(27) Rienstra-Kiracofe, J. C.; Tschumper, G. S.; Schaefer, H. F., III. *Chem. Rev.* **2002**, *102*, 231.
(28) Taylor, T. R.; Asmis, K. R.; Xu, C.; Neumark, D. M. *Chem. Phys. Lett.* **1998**, *297*, 133−140.
(29) Pelletier, J.; Gervais, D.; Pomot, C. *J. Appl. Phys.* **1984**, *55*, 994−1002.
(30) Vurgaftman, I.; Meyer, J. R. *Appl. Phys. Rev.* **2001**, *89*, 5815−5875.
(31) Sowers, A. T.; Christman, J. A.; Bremser, M. D.; Ward, B. L.; Davis, R. F.; Nemanich, R. J. *Appl. Phys. Lett.* **1997**, *71*, 2289−2291.
(32) Forsythe, E. M.; Sprague, J. A.; Khan, B. A.; Metha, S.; Smith, D. A.; Murzin, I. H.; Ahern, B.; Weyburne, D. W.; Tompa, G. S. *Mater. Res. Soc. Symp. Proc.* **1997**, *449*, 1233−1238.